Hindawi
Advances in Civil Engineering
Volume 2023, Article ID 6667430, 17 pages
https://doi.org/10.1155/2023/6667430

Research Article

Study on the Division of the Affected Zone under Construction Unloading and Its Construction Sequence of the Multiline Parallel River-Crossing Pipe Jacking

Zhang Ziguang,[1] **Mao Ruijin**,[1] **Zhang Jiesheng**,[2] **Wang Xuefeng**,[1] **and Zhang Mengqing**[1]

[1]*Anhui Province Key Laboratory of Building Structure and Underground Engineering, Anhui Jianzhu University, Hefei, China*
[2]*The First Engineering Co., Ltd. CTCE Group, Hefei, China*

Correspondence should be addressed to Zhang Ziguang; phdzzg@ahjzu.edu.cn

Received 12 February 2023; Revised 3 June 2023; Accepted 8 June 2023; Published 30 June 2023

Academic Editor: Jianyong Han

There are many advantages of reasonably determining the affected zone and its construction sequence for the multiline parallel pipe-jacking construction, such as convenient to reasonably arrange the pipeline section distribution mode, reducing the construction safety risk, and construction difficulty. Combined with the engineering construction practice of the multiline parallel pipe-jacking project for the north city drainage and flood control project through Chu River in Hefei, the strength reduction method has been utilized to study the surrounding stratum FOS for the pipe-jacking construction unloading under different overburden thickness Hs, different clear distance D, and different river water depth H_w in this paper. The formula of the minimum critical overburden thickness $Hs_{\min}$ and the minimum critical clear distance $D_{\min}$ of the surrounding stratum self-stability during pipe-jacking construction unloading have been derived. The division method of the affected zone for the multiline parallel river-crossing pipe-jacking construction which behaves as the mutual influence nonself-stability zone, the mutual influence self-stability zone, and the no mutual influence self-stability zone has been proposed. For further discussion, the construction sequence of the multiline parallel river-crossing pipe jacking has been studied.

1. Introduction

Because of many advantages such as the little impact on the environment, the small construction area, the fast construction speed, and the high degree of mechanization, slurry balance pipe jacking has become an important construction method of underground pipeline construction through rivers, roads, buildings, etc. [1–4]. Due to the factors of the topographical conditions, functional requirements, and others, there are more and more multiline parallel pipe-jacking projects with small clear distance D and thin overburden thickness Hs, such as four parallel pipe jacking under the Guan River [5, 6] and three-hole parallel adjacent jacking in the drainage project of Meilan International Airport [7]. The construction process of multiline parallel pipe jacking is the mechanical process in which an incomplete structure with a gradual change in geometric shape and material properties is subjected to the change in construction loads in time and space. Early construction pipe jacking will impact on the surrounding environment of postconstruction pipe jacking by influencing the displacement and stress of its surrounding strata, while postconstruction pipe jacking will impact on early construction pipe jacking that has been completed during the construction process [8–12]. The repeated cross influence of multiple construction for multiline parallel pipe jacking will make the stress repeatedly adjusted and form the stress field closely related to the spatial distribution of pipe jacking with a significant space-time effect and group-hole effect [13, 14]. They have important theoretical significance and engineering application value to explore the self-stability ability of the surrounding strata during the construction of multiline parallel pipe jacking and define the reasonable construction sequence.

The main methods for studying on the surrounding stratum self-stabilizing capacity and the deformation characteristics of the multiline parallel pipe-jacking construction include the theoretical analysis method [15–19],

model test method [20, 21], in situ test method [22, 23], and numerical computational method [24–29]. At present, the numerical calculation method has become an increasingly important tool in urban underground engineering research due to its advantages of the high speed, high accuracy, low cost, time-saving and labor-saving, and strong adaptability to complex conditions and processes. The finite element strength reduction method (FESRM) is one of the numerical calculation methods. Because of many advantages of the strict mechanical basis, such as being quantifiable, visible, dynamic, and intuitive, FESRM has been widely used in the self-stability evaluation of surrounding rock stability of tunnels and underground projects in recent years [30–36].

At present, the research on the multiline parallel pipe-jacking construction mainly focuses on the deformation of surrounding strata and pipe-jacking segments, construction parameters, and other aspects. The research on the subject of the affected zone and construction sequence is mainly carried out in combination with specific projects, which is not systematic. Combined with engineering construction practice of the multiline parallel pipe-jacking project for the north city drainage and flood control project through Chu River in Hefei China, the strength reduction method has been utilized to study the surrounding stratum FOS for pipe-jacking construction unloading under different overburden thickness *Hs*, different clear distance *D*, and different river water depth H_w. The affected zone division idea and the construction sequence determination method of multiline parallel pipe-jacking construction are summarized and improved in this paper. The research results provide a case support and the theoretical basis for the multiline parallel river-crossing pipe-jacking construction with the thin overburden thickness and the narrow clear distance.

2. Mechanics and Engineering Profile

2.1. Mechanical Mechanism of Multiline Parallel Pipe-Jacking Construction. The construction method of slurry balance pipe jacking is carried out by using the pipe-jacking machine located in the starting well through the main pushing system. The cutter head of the pipe-jacking machine cuts the stratum in front of the pipe-jacking face and then discharges the stratum soil through the mud treatment system and transportation system. At the same time, under the continuous pushing of the main pushing system, the subsequent segments are pushed following the pipe-jacking machine one by one, until reaching the receiving well. In addition, the drag reduction slurry shall be properly injected behind the pipe-jacking segment according to the actual situation, and the whole pipe-jacking construction process is completed. The acting force acted on surrounding strata during pipe-jacking construction mainly includes the jacking force acting on the position of the pipe-jacking face and the frictional force between the pipe-jacking segment and the surrounding strata, as shown in Figure 1. When the pipe-jacking project is under normal construction, the stratum stress state near the pipe-jacking head in front of the machine is extremely complex due to the effect of the pipe-jacking force. The stratum stress state in front of the pipe-jacking machine increases due to the extrusion effect of the front additional thrust of the pipe-jacking face. After the pipe-jacking machine passes, as the outer diameter of the pipe-jacking machine is slightly larger than the outer diameter of the pipe segment, the stratum loss is formed between the subsequent pipe segment and the surrounding strata. The stratum moves towards the gap, and then, stress diffusion occurs. Simultaneous grouting behind the pipe segment causes the surrounding strata to be encapsulated. When pipe-jacking construction is completed, the surrounding stratum consolidation settlement will produce under the action of weight. During the whole process of pipe-jacking construction, the stress states of the pipe-jacking strata around are in a continuous dynamic change, which causes the continuous change of stratum displacement. When the overburden thickness is thin, the deformation of the strata around the pipe extends to the surface and causes surface deformation.

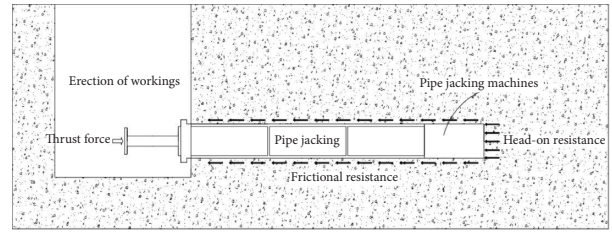

Figure 1: Mechanical principle of pipe-jacking construction.

When the clear distance between the early and the later stages of pipe-jacking construction is large, the stratum disturbance during the early stage has no impact on the later stage; meanwhile, the disturbance of the strata during the later stage has no impact on the early stage. When the clear distance between the early and the later stages of pipe-jacking construction is small, the later stage of pipe-jacking construction is completed in the strata affected by the disturbance of the early stage. At the same time, the stratum disturbance generated by the later stage has an impact on the early stage. The mutual influence degree becomes stronger as the clear distance decreases. When the clear distance between multiple parallel pipe-jacking is small, the change in the stratum stress state has been caused by the second pipe-jacking construction generating additional stress on the surrounding stratum of the first pipe jacking, which will change the stress and displacement. This effect is greater on the side close to each other and less on the side far away from each other, as shown in Figure 2(a). The third pipe-jacking construction has the same phenomenon, which generates the new equilibrium state and reacts on the first pipe jacking, the second pipe jacking, and the third pipe jacking through the stress state. Among them, the impact between two jacking pipes is greater when they are close to each other and less when they are far away from one side, as shown in Figure 2(b). In this case, three construction sequence problems arise (see Figure 3). When there are 4 pipe-jacking operations, the relative position relationship between pipes increases to 6 forms. When there are *n*pipe-jacking operations, the relative position relationships between pipes increase to C^2_n forms.

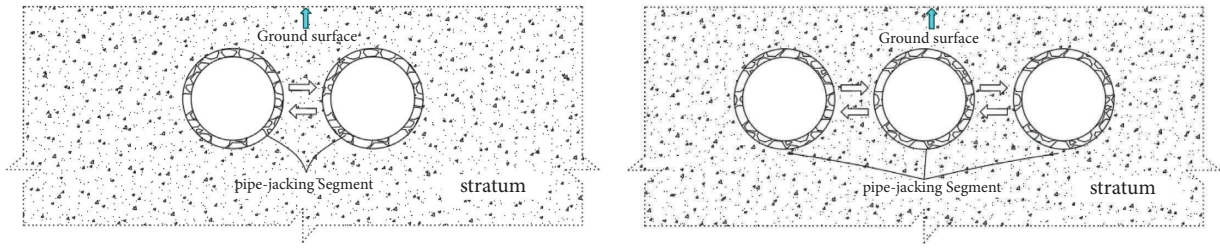

Figure 2: Interaction mechanism of multiline parallel pipe-jacking construction: (a) two-line pipe jacking; (b) three-line pipe jacking.

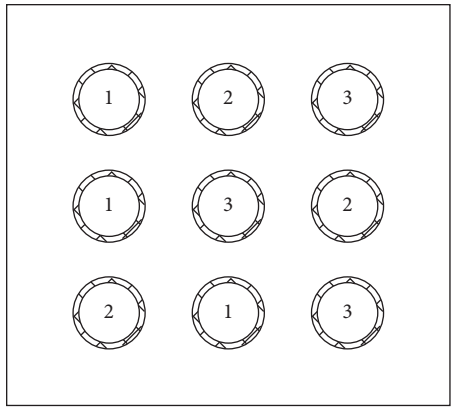

Figure 3: Construction sequence working conditions.

2.2. Project Overview. The north city drainage and flood control project is located in Hefei, China. The total length of the project line is 7015 m. Y25-Y26 of this project pipeline network crosses the main channel of Chu River. In this section, the width of the river channel is 55 m, the width is 25 m, the embankment height is 9.46 m, the slope is 45°, and the river depth is in the range of 2.0~5.0 m, as shown in Figure 4(a). Slurry balance mechanical pipe-jacking construction is adopted. Three circular reinforced concrete pipes with an inner diameter of 3.0 m and an outer diameter of 3.6 m are used for pipe jacking. The clear distance between two adjacent pipe jacking is 2.8 m. The stratum where pipe jacking crosses is silty clay. The thickness of the pipe-jacking covering layer in the riverbed section is 3.0 m, as shown in Figure 4(b). The vertical horizontal distance from the riverside of the pipe-jacking working shaft to the edge of the valley is about 10 m.

The project site belongs to the undulating plain landform of Jianghuai, and the microgeomorphology is the hillock with a concave groove. The regional geological structure belongs to the southern edge of the North China Plateau, and the secondary tectonic unit belongs to the Hefei Basin. The stratum distribution from top to bottom is as follows: fill soil, 0.5–1.5 m; silty chalky clay, 1.2–2.7 m; clay, 5.9–7.5 m; chalky clay, 4.8–6.0 m; and strongly weathered mudstone, 1.7–2.6 m, and the following are medium and slightly weathered mudstones. The physical and mechanical parameters of each stratum are shown in Table 1.

3. Study on the Division of the Affected Zone under Construction Unloading of Multiline Parallel River-Crossing Pipe Jacking

3.1. Research Methodology

3.1.1. Finite Element Strength Reduction Method. Due to the high aspect ratio, the problem of multiline parallel pipe-jacking construction unloading can be considered as a plain-strain one. The failure complies with the Mohr–Coulomb criterion which can be expressed as shown in the following formula:

$$F = \frac{1}{3} I_1 \sin\varphi + \left(\cos\theta_\sigma - \frac{1}{\sqrt{3}} \sin\theta_\sigma \sin\varphi \right) \sqrt{J_2} - c\cos\varphi = 0,$$
$$-\frac{\pi}{6} \le \theta_\sigma \le \frac{\pi}{6}, \tag{1}$$

where I_1 is the first invariant of the stress tensor, J_2 is the second invariant of the partial stress tensor, c is cohesion, φ is the angle of internal friction, and θ_σ is Lodder's angle.

The finite element strength reduction method (FESRM) is a method that combines the strength reduction technique, the principle of ultimate equilibrium, and the principle of elastic-plastic finite element calculations. First, the state of force and deformation under the original parametric working condition of the stratum was calculated. Then, the stratum strength parameters c and φ were simultaneously discounted according to equation (2) to obtain a new set of strength parameters c' and φ', and they were used as the new material strength parameters for calculation. Finally, the calculation was carried out by continuously adjusting the

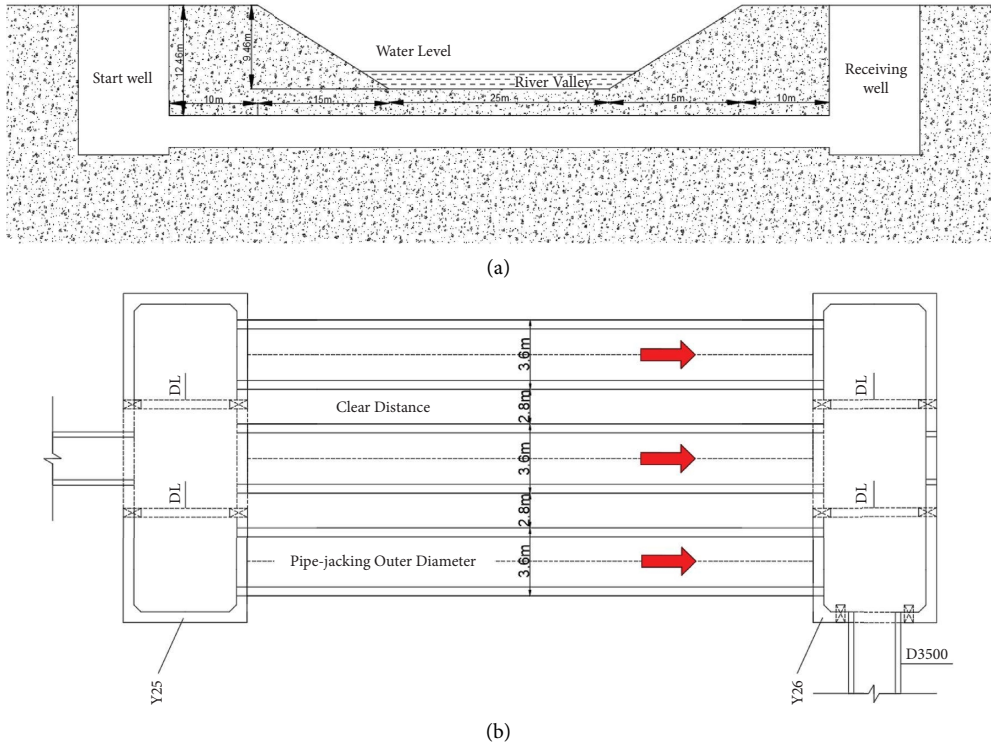

Figure 4: Engineering characteristic drawing of pipe jacking: (a) longitudinal section; (b) schematic plan.

Table 1: Physical and mechanical parameters of the strata.

Stratigraphic type	Elastic modulus E (Mpa)	Poisson's ratio	Heavy γ (kN/m^3)	Cohesion c (kPa)	Friction angle φ (°)	Thickness (m)
Fill soil	8.0	0.27	18.00	10	10.0	0.5~1.5
Silty, powdery clay	3.2	0.27	17.52	6.2	5.8	1.2~2.7
Clay	12.0	0.25	19.22	70	16.9	5.9~7.5
Powdery clay	11.3	0.25	19.22	40	15.5	4.8~6.0
Strongly weathered mudstone	25.0	0.35	22.00	90	30	1.7~2.6

discount factor k until the surrounding strata were in ultimate equilibrium, and the critical rupture surface was obtained; at the same time, the discount factor k of the material was FOS. The calculation principle of FESRM [23] is shown in Figure 5:

$$c' = \frac{c}{k},$$
$$\phi' = \arctan\left(\frac{\tan\phi}{k}\right), \tag{2}$$

where k is the discount factor.

3.1.2. Computational Model. Finite element numerical calculation software of Midas GTS NX was utilized to study the surrounding stratum self-stability characteristics of the pipe-jacking construction. The numerical calculation was based on the plane strain problem. Pipe jacking took a circle with an outer diameter of 3.6 m. The distance between the left and the right boundaries of the calculation model was more than 3 times of the pipe-jacking outer diameter, and the horizontal displacement constraint was applied. The distance between the lower boundary and the bottom of the

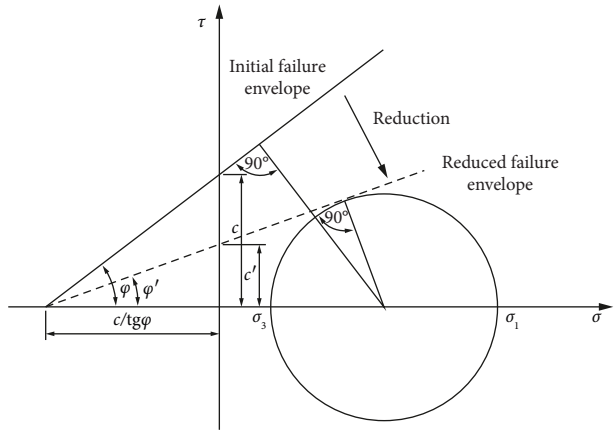

Figure 5: Calculation principle of SRM.

calculation model was more than 3 times of the pipe-jacking outer diameter, and the vertical displacement constraint was applied to the lower boundary, with the upper surface free. The model boundary calculation cell grid was set to 1.0 m longitudinally and horizontally, and the pipe perimeter grid was 0.5 m, as shown in Figure 6. The calculation used the DP4 equivalence Mohr–Coulomb yield criterion. Jacking construction unloading took place in the one-time full-section excavation. The initial stress took into account the self-weight of the ground soil and river water pressure, and no other construction process factors were considered. Numerical calculations of the physical and mechanical parameters of the strata, the dimensions of pipe jacking, and the relative position relationships were based on dependent engineering parameters as basic data and were extended to the general case on this basis. The method of controlling single variable analysis was adopted while discussing the self-stability characteristics of the unloading stratum during pipe-jacking construction; that is, when one calculation parameter changed, other calculation parameters remained unchanged.

3.2. Study on the Surrounding Stratum Self-Stability Characteristics of the Single-Line Pipe-Jacking Construction. In this study, H_w was taken as 2.0 m, 5.0 m, and 8.0 m, respectively, and the stratum of pipe-jacking crossing was silty clay stratum. The FOS calculation results of the pipe-jacking construction surrounding strata under different *Hs* are shown in Table 2.

From Table 2, it was shown that the overall change trend of FOS increased first and then decreased with an increase in *Hs* under the same conditions of other factors (see Figure 7). It illustrated the problem of the surrounding stratum self-stabilizing ability for pipe-jacking construction increased first and then decreased with an increase in *Hs*. The fundamental reason for the above phenomenon was that the self-stability characteristics of the pipe-jacking construction surrounding strata were mainly determined by the relative relationship between the stratum strength itself and the surrounding stratum redistribution stress caused by pipeline construction unloading. The surrounding stratum redistribution stress by pipeline construction unloading was positively related to the stratum initial stress itself under the same conditions of other factors. The stratum initial stress was composed of the effect for stratum self-weight and for the river water self-weight. With an increase in stratum depth, the effect of the former on the stratum initial stress gradually increased, while the latter gradually decreased. Thus, the stratum initial stress decreased first and then increased with an increase in stratum depth. Furthermore, the surrounding stratum redistribution stresses the same rule. The stratum strength itself was basically unchanged. Therefore, the ratio of stratum strength to the surrounding stratum redistribution stress increased first and then decreased.

FOS could quantitatively evaluate the degree of surrounding stratum self-stability by pipe-jacking construction unloading. Taking FOS = 1.25 as limitation, the calculation

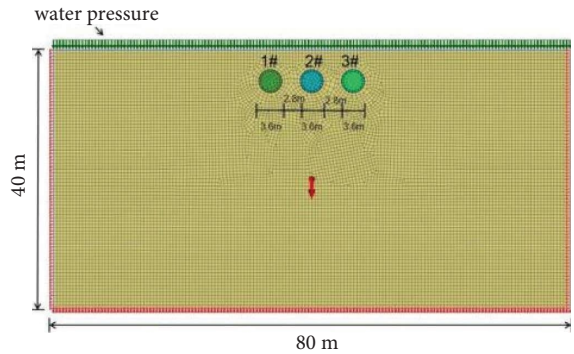

Figure 6: Calculation model.

Table 2: FOS calculation results.

H_w = 2.0 m		H_w = 5.0 m		H_w = 82.0 m	
Hs (m)	FOS	*Hs* (m)	FOS	*Hs* (m)	FOS
0.1	1.05	0.1	—	0.1	—
0.2	1.45	0.2	—	0.2	—
0.5	1.80	0.5	1.05	0.5	1.01
1.0	2.06	1.0	1.31	1.0	1.01
1.5	2.10	1.5	1.42	1.5	1.13
2.0	2.03	2.0	1.48	2.0	1.23
2.5	1.95	2.5	1.53	2.5	1.28
3.0	1.90	3.0	1.50	3.0	1.31
6.0	1.63	6.0	1.45	6.0	1.33
12.0	1.38	12.0	1.31	12.0	1.24
18.0	1.23	18.0	1.20	18.0	1.18
24.0	1.17	24.0	1.15	24.0	1.12
30.0	1.12	30.0	1.10	30.0	1.09
36.0	1.08	36.0	1.06	36.0	1.06
42.0	1.06	42.0	1.03	42.0	1.04

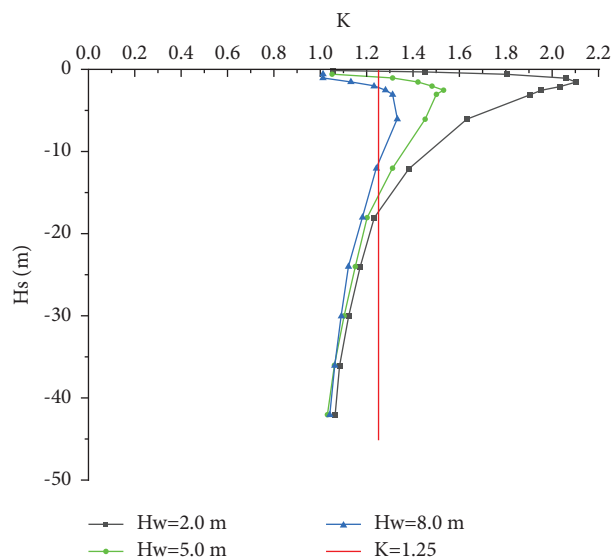

Figure 7: FOS changed with *Hs*.

results of the surrounding stratum minimum critical overburden thickness Hs_{min} *d*, the maximum critical overburden thickness Hs_{max} *r*, and the single-line pipe-

jacking construction under different river water depth H_w are shown in Table 3. The mathematical fitting equations between $Hs_{\min}$ H_w and $Hs_{\max}$ H_w are shown in equations (3) and (4), respectively:

$$Hs_{\min} = 0.04536H_w^2 + 0.1025\,H_w - 0.22286, \quad R^2 = 0.98771, \tag{3}$$

$$Hs_{\max} = 0.1525H_w^2 + 0.58893\,H_w - 16.21071. \quad R^2 = 0.99386. \tag{4}$$

The basic goal of an excellent underground space development plan was to make full use of the stratum self-stability ability, minimize the engineering auxiliary measures, and pay attention to the economy while ensuring safety. The realization of this goal mainly depends on the geological conditions of the site, the understanding of these geological conditions, and the ability to use them as design. Taking $Hs_{\min}$ $Hs_{\max}$ as the upper and the lower limitation, respectively, the surrounding stratum self-stability distribution zone of single-line pipe-jacking construction unloading is shown in Figure 8. For the specific environmental conditions of pipe-jacking construction, there are many advantages for the pipe-jacking vertical section that was designed in the surrounding stratum self-stability distribution zone, such as reducing the construction safety risk and construction difficulty.

3.3. Study on the Surrounding Stratum Self-Stability Characteristics for the Two-Line Parallel Pipe-Jacking Construction. In this study, H_w was taken as 2.0 m, 5.0 m, and 8.0 m, respectively, Hs was taken as 3.0 m, and the stratum of pipe-jacking crossing was the silty clay stratum. The FOS calculation results of the pipe-jacking construction surrounding strata under different D are shown in Table 4.

From Table 4, it was shown that the overall change trend of FOS increased first and then decreased with an increase in D under the same conditions of other factors (see Figure 9). With an increase in D, the potential failure pattern of the surrounding strata for double-line parallel pipe-jacking construction unloading transited from the double pipe-jacking overall collapse to the gradual separation collapse, and the final collapse pattern was consistent with that of single pipe-jacking (see Figure 10). It was demonstrated that when D was small, the mutual influence was strong of double-line parallel pipe-jacking construction unloading. With D increased, the mutual influence was gradually weakened, and when D increased to a certain extent, it would be no longer affecting each other.

Taking FOS = 1.25 as the limitation, the calculation results of the surrounding stratum minimum critical clear distance $D_{\min}$ for the double-line pipe-jacking construction under different buried depths Hs are shown in Table 5. The mathematical fitting equation among the minimum critical clear distance $D_{\min}$, the overburden thickness Hs, and the river water depth H_w of double-line parallel pipe-jacking construction unloading is shown in equation (5). The spatial

Table 3: Surrounding stratum critical overburden thickness.

H_w (m)	2.0	3.0	4.0	5.0	6.0	7.0	8.0
$Hs_{\min}$	0.15	0.41	0.57	0.72	1.30	1.72	2.31
$Hs_{\max}$	16.8	16.71	15.86	15.38	14.37	12.93	11.08

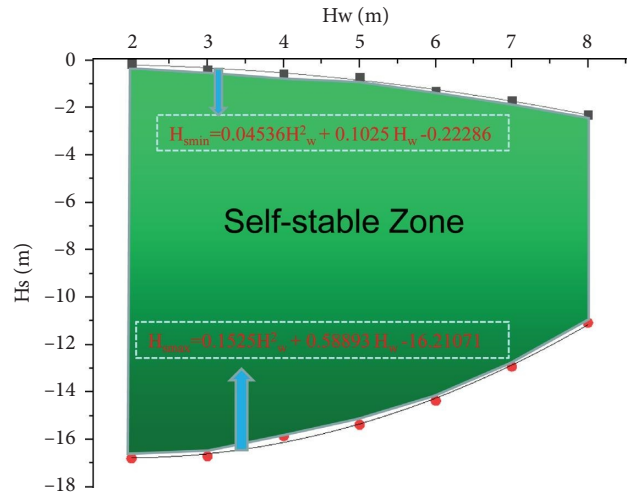

Figure 8: Surrounding stratum self-stability distribution zone.

Table 4: FOS calculation results.

$H_w = 2.0$ m		$H_w = 5.0$ m		$H_w = 8.0$ m	
D (m)	FOS	D (m)	FOS	D (m)	FOS
1.0	1.15	1.0	1.05	1.0	—
2.0	1.32	2.0	1.08	2.0	—
3.0	1.46	3.0	1.19	3.0	1.01
4.0	1.58	4.0	1.30	4.0	1.11
5.0	1.68	5.0	1.40	5.0	1.20
6.0	1.78	6.0	1.45	6.0	1.27
7.0	1.83	7.0	1.48	7.0	1.29
8.0	1.88	8.0	1.50	8.0	1.30
9.0	1.88	9.0	1.50	9.0	1.30

feature distribution map among them is drawn in Figure 11, which provided the theoretical basis for the cross-sectional design of the multiline parallel pipe-jacking construction:

$$D_{\min} = -0.26163 + 0.33132H_s + 0.45693H_w + 0.0533H_s^2 + 0.03489H_sH_w + 0.00658H^2, \quad R^2 = 0.99888. \tag{5}$$

3.4. Study on the Surrounding Stratum Self-Stability Characteristics for the Three-Line Parallel Pipe-Jacking Construction. In this study, H_w was taken as 2.0 m, 5.0 m, and 8.0 m, respectively, Hs was taken as 3.0 m, and the stratum of pipe-jacking crossing was the silty clay stratum. Three working conditions were taken for the construction sequence, which were 1# ⟶ 2# ⟶ 3#, 2# ⟶ 1# ⟶ 3#,

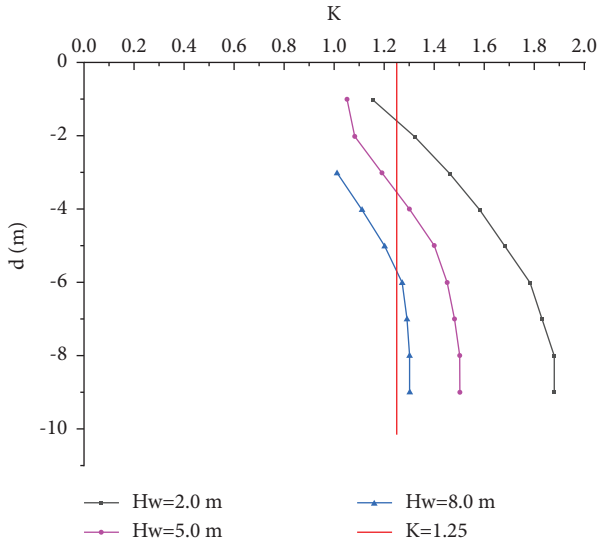

Figure 9: FOS changed with *Hs*.

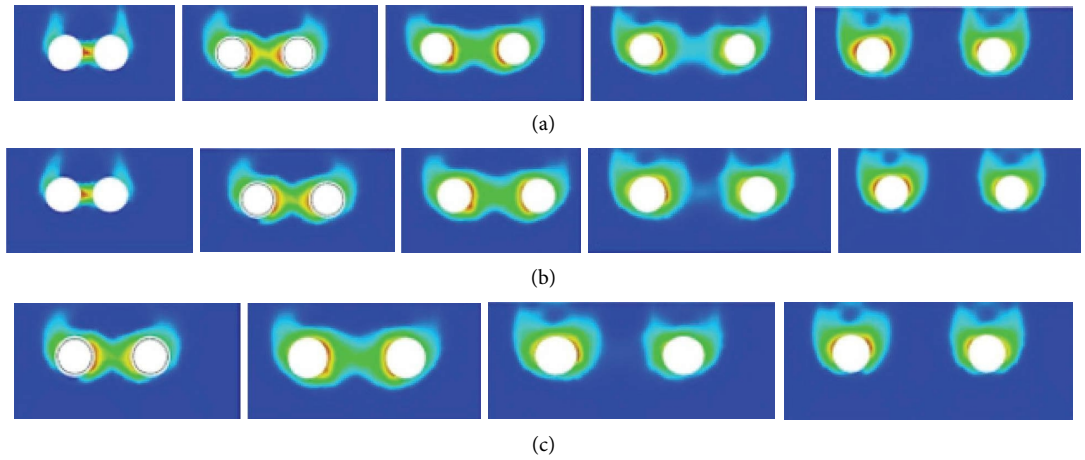

Figure 10: Potential fracture surface for typical working conditions: (a) $H_w = 2.0$ m (D was 1 m, 3 m, 5 m, 7 m, and 9 min sequence); (b) $H_w = 5.0$ m (D was 1 m, 3 m, 5 m, 7 m, and 9 min sequence); (c) $H_w = 8.0$ m (D was 3 m, 5 m, 7 m, and 9 min sequence).

Table 5: Surrounding stratum critical clear distance D_{min}.

Hs (m)		1.0	2.0	3.0	4.0	5.0 m	6.0	7.0	8.0 m
	2.0	1.00	1.18	1.52	2.00	2.64	3.60	4.25	5.80
H_w (m)	5.0	2.83	3.00	3.56	4.27	5.18	6.23	7.37	8.63
	8.0	—	—	5.71	6.84	7.86	9.09	10.24	11.92

and 1# ⟶ 3# ⟶ 2# (see Figure 9). The FOS calculation results of the pipe-jacking construction surrounding strata under different D are shown in Table 6.

From Table 4, it was shown that with the pipe-jacking number increased, FOS tends to decrease gradually on the whole, and the smaller the D was, the more significant the trend was. When the pipe-jacking construction was completed, FOS was not affected by the construction sequence. However, when the sequence was different, FOS in the construction process was different (see Figure 12). The overall change trend of FOS increased first and then decreased with an increase in D under the same conditions of other factors (see Figure 13). With an increase in D, the potential failure pattern of the surrounding strata for three-line parallel pipe-jacking construction unloading transited from the double pipe-jacking overall collapse to the gradual separation collapse, and the final collapse pattern was consistent with that of single pipe jacking (see Figure 14). It was demonstrated that when D was small, the mutual influence was strong of three-line parallel pipe-jacking construction unloading; with D increased, the mutual influence was gradually weakened, and when D increased to a certain extent, it would be no longer affecting each other.

Taking FOS = 1.25 as the limitation, the calculation results of the surrounding stratum minimum critical clear distance D_{min} for the three-line pipe-jacking construction under different buried depths *Hs* are shown in Table 7. The mathematical fitting equation among the minimum critical clear distance D_{min}, the overburden thickness *Hs*, and the

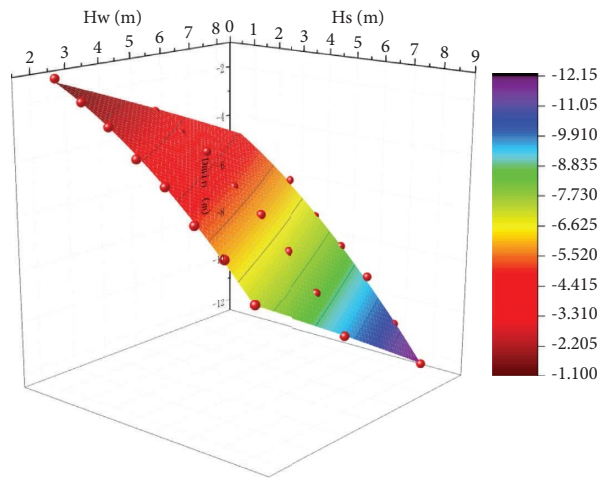

Figure 11: Spatial feature distribution map.

Table 6: FOS calculation results.

H_w (m)	D (m)	1#-2#-3#			2#-1#-3#			1#-3#-2#		
2.0	1.0	1.85	1.18	1.15	1.85	1.18	1.00	1.85	1.70	1.00
	2.0	1.85	1.32	1.18	1.85	1.32	1.18	1.85	1.85	1.18
	3.0	1.85	1.45	1.37	1.85	1.40	1.35	1.85	1.85	1.35
	4.0	1.85	1.58	1.50	1.85	1.58	1.50	1.85	1.85	1.50
	5.0	1.85	1.70	1.65	1.85	1.68	1.65	1.85	1.85	1.64
	6.0	1.85	1.80	1.75	1.85	1.78	1.74	1.85	1.85	1.75
	7.0	1.85	1.83	1.83	1.85	1.83	1.84	1.85	1.85	1.84
	8.0	1.85	1.85	1.85	1.85	1.85	1.85	1.85	1.85	1.85
	9.0	1.85	1.85	1.85	1.85	1.85	1.85	1.85	1.85	1.85
5.0	2.0	1.50	1.08	1.01	1.50	1.08	1.00	1.50	1.50	1.02
	3.0	1.50	1.19	1.10	1.50	1.19	1.11	1.50	1.50	1.11
	4.0	1.50	1.30	1.24	1.50	1.30	1.25	1.50	1.50	1.24
	5.0	1.50	1.40	1.38	1.50	1.40	1.37	1.50	1.50	1.37
	6.0	1.50	1.45	1.44	1.50	1.45	1.43	1.50	1.50	1.44
	7.0	1.50	1.50	1.48	1.50	1.50	1.49	1.50	1.50	1.49
	8.0	1.50	1.50	1.49	1.50	1.50	1.50	1.50	1.50	1.50
	9.0	1.50	1.50	1.50	1.50	1.50	1.50	1.50	1.50	1.50
8.0	3.0	1.30	1.03	1.03	1.30	1.03	1.00	1.30	1.30	1.00
	4.0	1.30	1.13	1.08	1.30	1.12	1.08	1.30	1.30	1.08
	5.0	1.30	1.20	1.18	1.30	1.20	1.18	1.30	1.30	1.19
	6.0	1.30	1.27	1.25	1.30	1.27	1.25	1.30	1.30	1.25
	7.0	1.30	1.29	1.29	1.30	1.29	1.29	1.30	1.30	1.29
	8.0	1.30	1.30	1.30	1.30	1.30	1.30	1.30	1.30	1.30
	9.0	1.30	1.30	1.30	1.30	1.30	1.30	1.30	1.30	1.30

river water depth H_w of double-line parallel pipe-jacking construction unloading is shown in equation (6). The spatial feature distribution map among them is drawn in Figure 15:

$$D_{\min} = 0.07265 - 0.20648H_s + 0.44784H_w + 0.08245H_s^2 + 0.06358H_sH_w + 0.00872H_w^2, \quad (6)$$
$$R^2 = 0.99874.$$

3.5. Dividing Mutual Influence Zones of Multiline Parallel Pipe-Jacking Construction Unloading. The surrounding stratum self-stability degree of multiline parallel pipe-jacking construction unloading could be determined quantitatively by FOS, and the mutual influence degree of them could be determined quantitatively by the change in FOS. For the convenience of expression, when the multiline parallel pipe-jacking construction has been completed, FOS was uniformly called FOS-M. Meanwhile, the single-line pipe-jacking construction has been completed, and FOS was uniformly called FOS-S. Taking FOS = 1.25 as the limitation, based on the surrounding stratum self-stability degree and the mutual influence degree, the surrounding stratum zone of the multiline parallel pipe-jacking construction unloading could be divided.

When FOS-M ≤ FOS-S < 1.25, it meant that the mutual influence would occur during multiline parallel pipe-jacking construction unloading, and the surrounding stratum zone

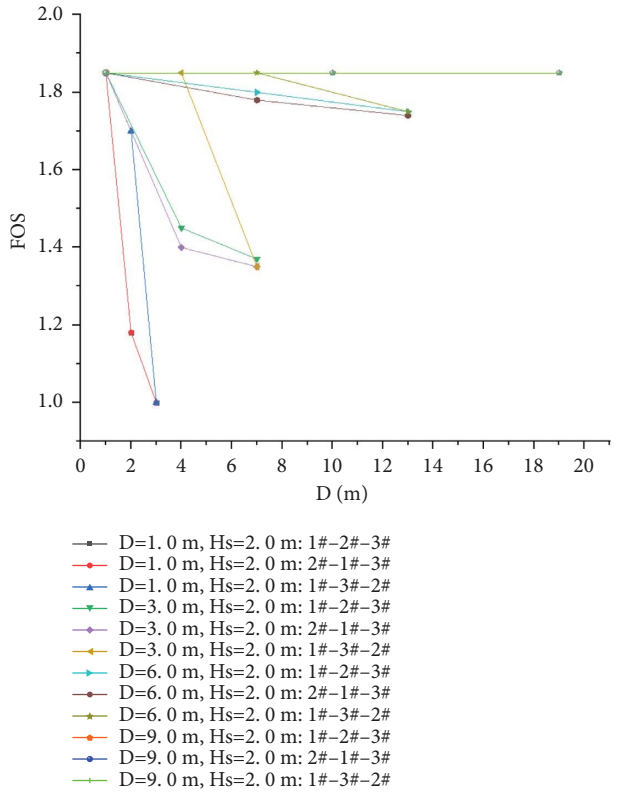

Figure 12: FOS changed with the construction process.

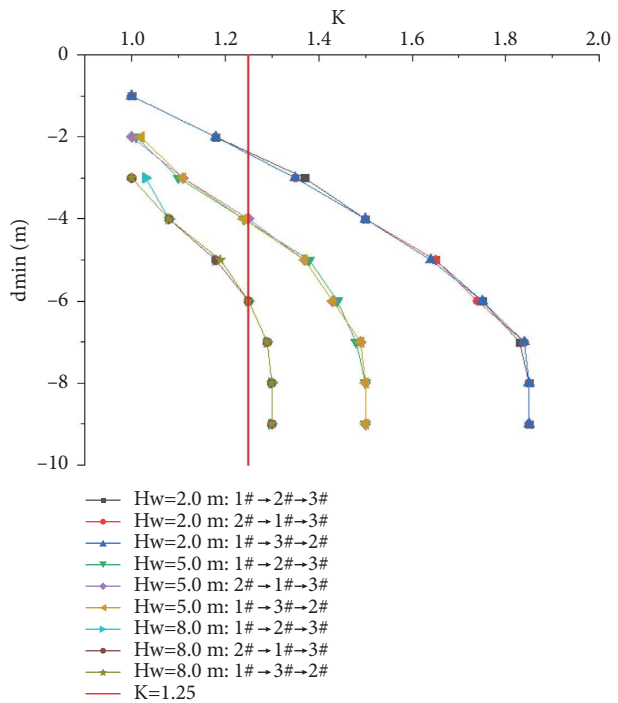

Figure 13: FOS changed with *Hs*.

did not meet the self-stability requirement. Thus, the surrounding stratum zone was called the mutual influence nonself-stability zone.

When 1.25 < FOS-M < FOS-S, it meant that the mutual influence would occur during multiline parallel pipe-jacking construction unloading, and the surrounding stratum zone

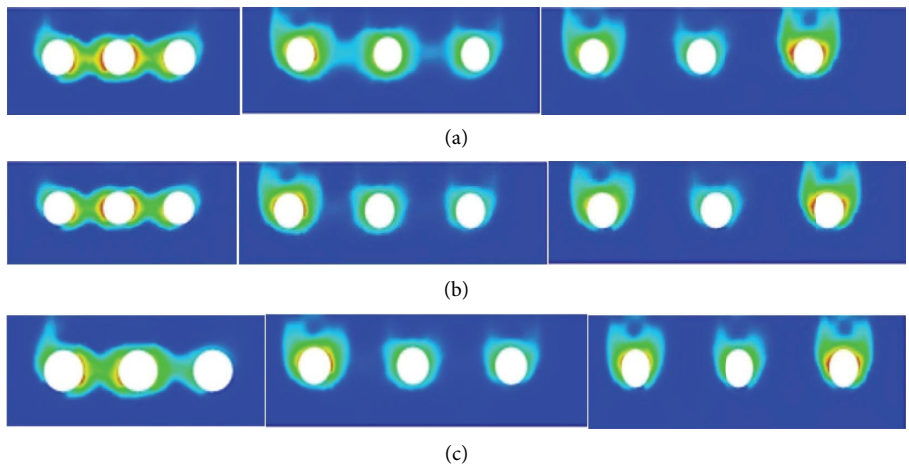

Figure 14: Potential fracture surface for typical working conditions: (a) $H_w = 2.0$ m (D was 3 m, 5 m, and 9 min sequence); (b) $H_w = 5.0$ m (D was 3 m, 5 m, and 9 min sequence); (c) $H_w = 8.0$ m (D was 3 m, 7 m, and 9 min sequence).

Table 7: Surrounding stratum critical clear distance D_{min}.

Hs (m)		1.0	2.0	3.0	4.0	5.0	6.0	7.0	8.0
H_w (m)	2.0	1.01	1.68	2.37	3.28	4.02	5.10	6.00	7.28
	5.0	2.86	3.51	4.02	5.13	5.95	7.08	8.37	9.66
	8.0	—	—	6.00	7.25	8.23	9.21	10.83	12.12

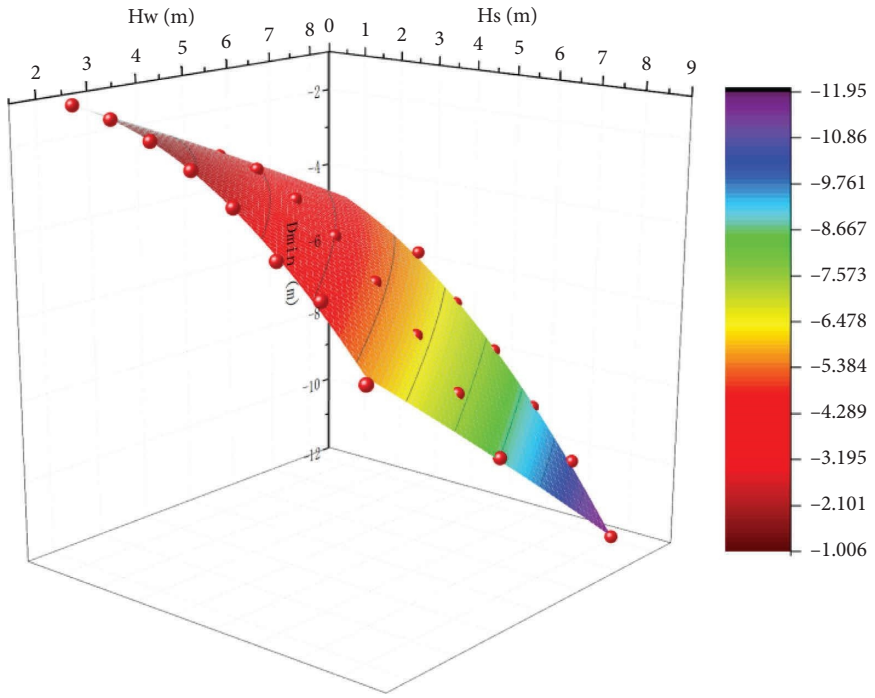

Figure 15: Spatial feature distribution map.

met the self-stability requirement. Thus, the surrounding stratum zone was called the mutual influence self-stability zone.

When FOS-M = FOS-S > 1.25, it meant that the mutual influence would not occur during multiline parallel pipe-jacking construction unloading, while the surrounding stratum zone met the self-stability requirement. Thus, the surrounding stratum zone was called the nonmutual influence self-stability zone.

4. Study on the Construction Sequence of the Multiline Parallel River-Crossing Pipe Jacking

4.1. Basic Assumptions. The stratum initial stress had been changed by pipe-jacking construction, which led to a series of complex physical and mechanical effects. It was not only related to the physical properties of the stratum but also closely related to the construction method, construction process, and relevant construction parameters. When using numerical software for calculation, it was difficult to take all factors into account to completely reflect the construction process. Therefore, proper simplification should be carried out during numerical calculation. It could not only meet the requirements of calculation software but also make the numerical calculation result reflect the construction process well.

According to the actual situation of the supporting project, the numerical calculation was based on the following assumptions in this paper:

(1) All strata were homogeneous, continuous, and isotropic ideal elastic-plastic material. The influence of groundwater is ignored in the calculation process. The initial stress only considers the stratum self-weight stress. Stratum settlement was only considered due to pipe-jacking construction, and the consolidation settlement was ignored.

(2) Jacking pressure of the pipe-jacking excavation surface was applied to the whole excavation surface in the form of a circular uniformly distributed load. The pressure was taken as the lateral static earth pressure at the center of the pipe-jacking excavation surface. According to the project actual situation, the pressure was 88.5 kpa in this paper, as shown in Figure 16(a).

(3) The influence of grouting pressure on the construction process was not considered. The grouting unit around pipe jacking was distributed along the radial and equal thickness of the segment. The elastic modulus was taken as 1/50 of the original formation unit, and the thickness of the grouting equivalent layer was 2 cm, as shown in Figure 16(b).

(4) The pipe joint material was an isotropic linear elastic body, and the indirect head effect of a pipe joint was ignored. The friction resistance between pipeline and stratum acted on the outer surface of the pipe casing and the inner surface of the soil around the pipe, with the same size and opposite direction. The frictional resistance was a certain value and evenly distributed along the pipe-jacking direction. The frictional resistance was achieved by setting a friction coefficient on the contact surface, and the value was 3.5 kpa in this paper, as shown in Figure 16(c).

4.2. Calculation Model and Implementation Process. The length, the width, and the height of the numerical calculation model for the multiline parallel pipe-jacking construction were 80 m, 80 m, and 30 m, respectively. The left and right boundaries of the calculation model were subject to horizontal displacement constraints, the lower boundary was subject to vertical displacement constraints, and the upper surface was free. The pipe-jacking segment was regarded as an elastic material, and the thickness was 0.30 m. The shell of the pipe-jacking machine adopted the linear elastic model. The material property adopted a 2D plate element, and the thickness was 0.06 m, as shown in Table 8. The material properties of strata and segments adopted 3D unit entities, which were divided into meshes by geometry and then expanded by 2D meshes. The calculation unit grid around pipe jacking was set to 0.5 m in both vertical and horizontal directions, while the model boundary was 2.0 m. The values of the stratum physical and mechanical parameters are shown in Table 1, and the calculation model is shown in Figure 17.

The numerical calculation process of the multiline parallel pipe-jacking construction was divided into the following stages: pipe-jacking excavation, pipe-jacking advance, and segment application. The specific steps were as follows: (1) The initial boundary conditions of the model and the stratum self-weight were applied, the initial displacement was cleared, and the analysis of the initial stress field was started. (2) The jacking pressure of the pipe-jacking face was applied, the function of the stratum excavated by pipe-jacking construction was deactivated, and the friction resistance was activated; at the same time, the casing of the pipe jacking machine was activated. (3) The shell of the pipe-jacking machine was deactivated, the pipe-jacking machine was jacked, and the pipe-jacking segment was applied. (4) The stratum of the next pipe segment was excavated, and the above steps were repeated.

4.3. Calculation and Analysis. There were differences in the degree of disturbance to the surrounding strata caused by the different jacking sequences of the multiline parallel pipe-jacking construction, which made the stratum displacement different. It was very important to control the stratum displacement by relying on the pipe-jacking project passing through the river channel. The cumulative vertical displacement of the stratum under various working conditions is shown in Figure 17. Displacement monitoring points were set at the river bottom surface section at the river center, which was perpendicular to the pipe-jacking axis. The surface displacement monitoring points directly above 1#, 2#, and 3# pipe jacking were marked as *S*1, *S*2, and *S*3 in turn (see Figure 18).

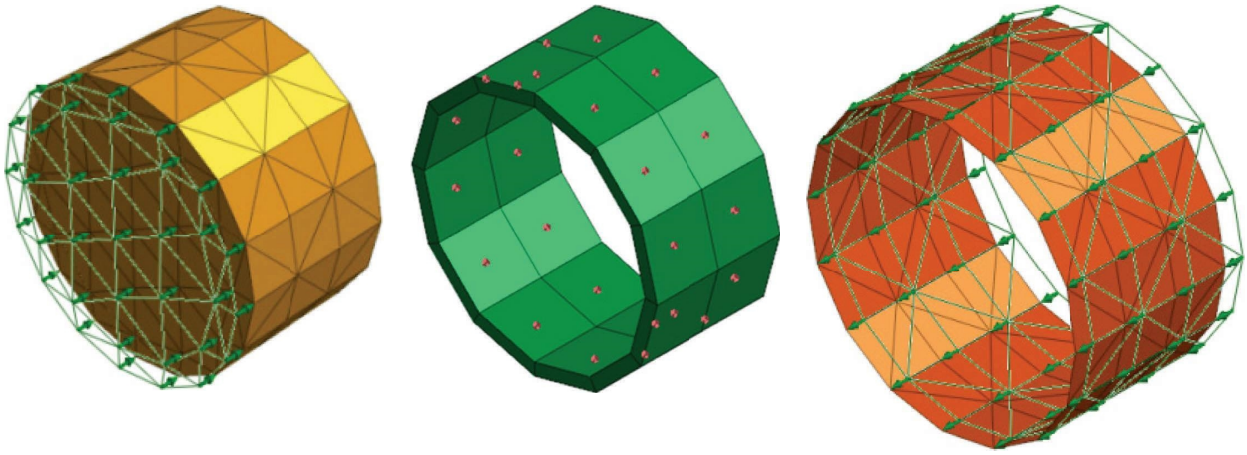

(a) (b) (c)

Figure 16: Numerical calculation assumption: (a) jacking pressure; (b) grouting equivalent layer; (c) frictional resistance.

Table 8: Calculation parameters.

Material type	Elastic modulus (Mpa)	Poisson ratio	Heavy γ (kN/m^3)	Thickness (m)
Pipe-jacking joints	28000	0.2	23	0.3
Topside shields	206000	0.3	78.5	0.06

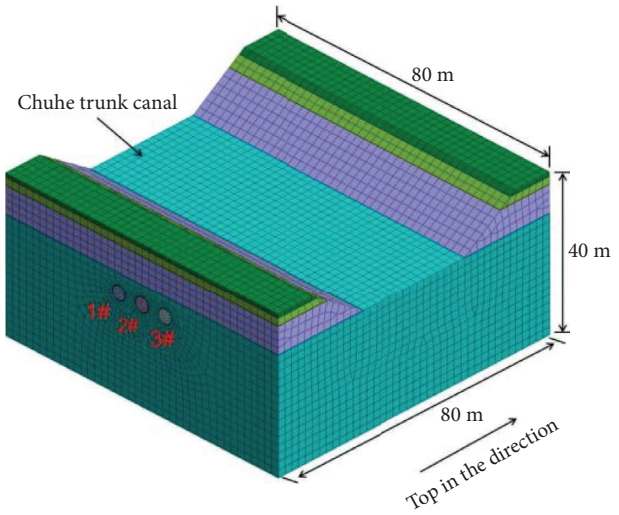

Figure 17: Calculation model.

The calculation results of the stratum deformation at *S*1, *S*2, and *S*3 points in the construction steps of the construction sequences for 1# ⟶ 2# ⟶ 3#, 2# ⟶ 1# ⟶ 3#, and 1# ⟶ 3# ⟶ 2# were extracted, respectively, as shown in Figure 19.

From Figure 19, it was shown that the overall law of stratum displacement at *S*1, *S*2, and *S*3 points in the construction steps under different construction sequences was basically consistent. On the whole, the stratum uplifted in the front of the pipe-jacking cutter head and subsided in the rear. The former was caused by the jacking force of the pipe-jacking face, and the latter was caused by the formation loss caused by the cutter head of the pipe-jacking machine slightly larger than the outer diameter of the segment. The mutual influence of stratum displacement was very strong caused by the three-line parallel pipe-jacking construction.

The calculation results of the pipe jacking in the construction sequence of "1# ⟶ 2# ⟶ 3#" were taken as examples for detailed explanation. During the construction of 1# pipe jacking, with the distance between the cutter head and the river center continuously approaching, the stratum displacement at *S*1, *S*2, and *S*3 was continuously uplifted and the value gradually increased. When the cutter head was pushed directly below the river center, the uplift of the stratum displacement at *S*1, *S*2, and *S*3 reached the maximum. When the cutter head passed through the river center, the stratum displacement at *S*1 rapidly sank to the negative value (settlement), and the displacement at *S*2 slightly sank. With the distance between the cutter head and the river center getting further away, the stratum displacement at *S*1, *S*2, and *S*3 was becoming slower and tending to be stable. During the construction of 2# pipe jacking, with the distance between the cutter head and the river center continuously approaching, the stratum displacement at *S*2 and *S*3 was continuously uplifted and the value gradually increased, while *S*1 showed the rising trend, but the value was small. When the cutter head was pushed directly below the river center, the uplift of the stratum displacement at *S*2 and *S*3 reached the maximum, while *S*1 rose to the maximum value. When the cutter head passed through the river center, the stratum displacement at *S*2 rapidly sank to a negative value (settlement), while *S*1 and *S*3 slightly sank. With the distance between the cutter head and the river center getting further away, the stratum displacement at *S*1, *S*2, and *S*3 was

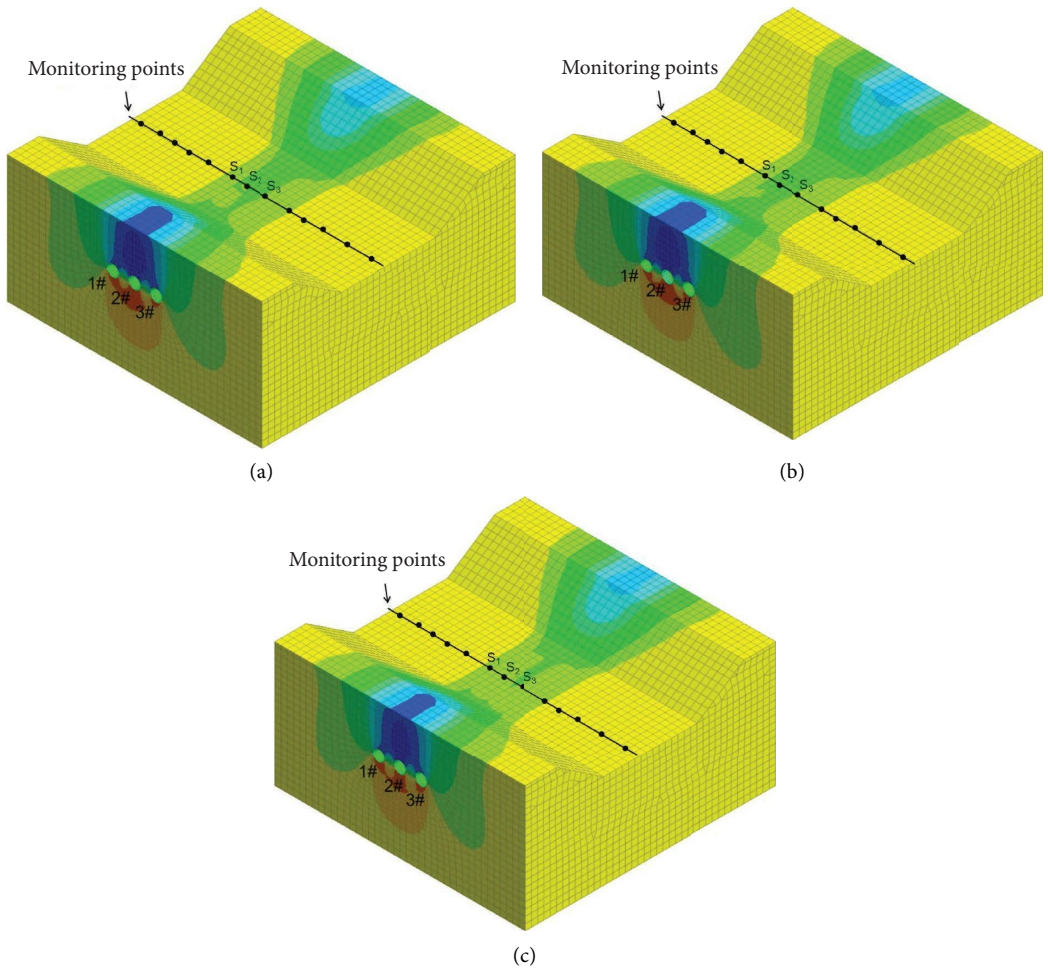

Figure 18: Surrounding stratum vertical displacement: (a) 1# ⟶ 2# ⟶ 3#; (b) 2# ⟶ 1# ⟶ 3#; (c) 1# ⟶ 3# ⟶ 2#.

becoming slower and tending to be stable. 3# pipe-jacking construction had little impact on the stratum displacement at *S*1. During the construction of 3# pipe-jacking, with the distance between the cutter head and the river center continuously approaching, the stratum displacement at *S*3 was continuously uplifted and the value gradually increased, while *S*2 showed the rising trend, but the value was small. When the cutter head was pushed directly below the river center, the uplift of the stratum displacement at *S*3 reached the maximum, while *S*2 rose to the maximum value. When the cutter head passed through the river center, the stratum displacement at *S*3 rapidly sank to a negative value (settlement), while *S*2 slightly sank. With the distance between the cutter head and the river center getting further away, the stratum displacement at *S*2 and *S*3 was becoming slower and tending to be stable.

When the first, the second, and the third pipe-jacking has been completed, respectively, in the sequence of 1# ⟶ 2# ⟶ 3#, 2# ⟶ 1# ⟶ 3#, and 1# ⟶ 3# ⟶ 2#, the calculation results of river bottom stratum deformation at the river bottom surface section in the river center, which was perpendicular to the pipe jacking axis, are shown in Figure 20.

From Figure 20, it is shown that the overall law of stratum displacement at the river center section under different construction sequences was basically consistent. The mutual influence of stratum displacement was very strong caused by the three-line parallel pipe-jacking construction. When the single-line pipe-jacking construction was completed, the horizontal surface displacement curve was approximately in a normal distribution. The maximum settlement was located at the pipe-jacking axis, and the maximum settlement value was 18.73 mm and gradually decreased from the axis to both sides. When the double-line pipe-jacking construction was completed and the clear distance *D* was narrow (in the sequence of 1# ⟶ 2# or 2# ⟶ 1#), the horizontal surface displacement curve showed the partial v-shaped distribution, and the surface settlement maximum value was 25.10 mm, which was located between two pipe jacking and in the pipe-jacking side that was constructed first. When the clear distance *D* was wide (in the sequence of 1# ⟶ 3# or 3# ⟶ 1#), the horizontal surface displacement curve showed the partial w-shaped distribution. When the three-line parallel pipe-jacking construction was completed in the sequence of 1# ⟶ 2# ⟶ 3#, 2# ⟶ 1# ⟶ 3#, and 1# ⟶ 3# ⟶ 2#, the

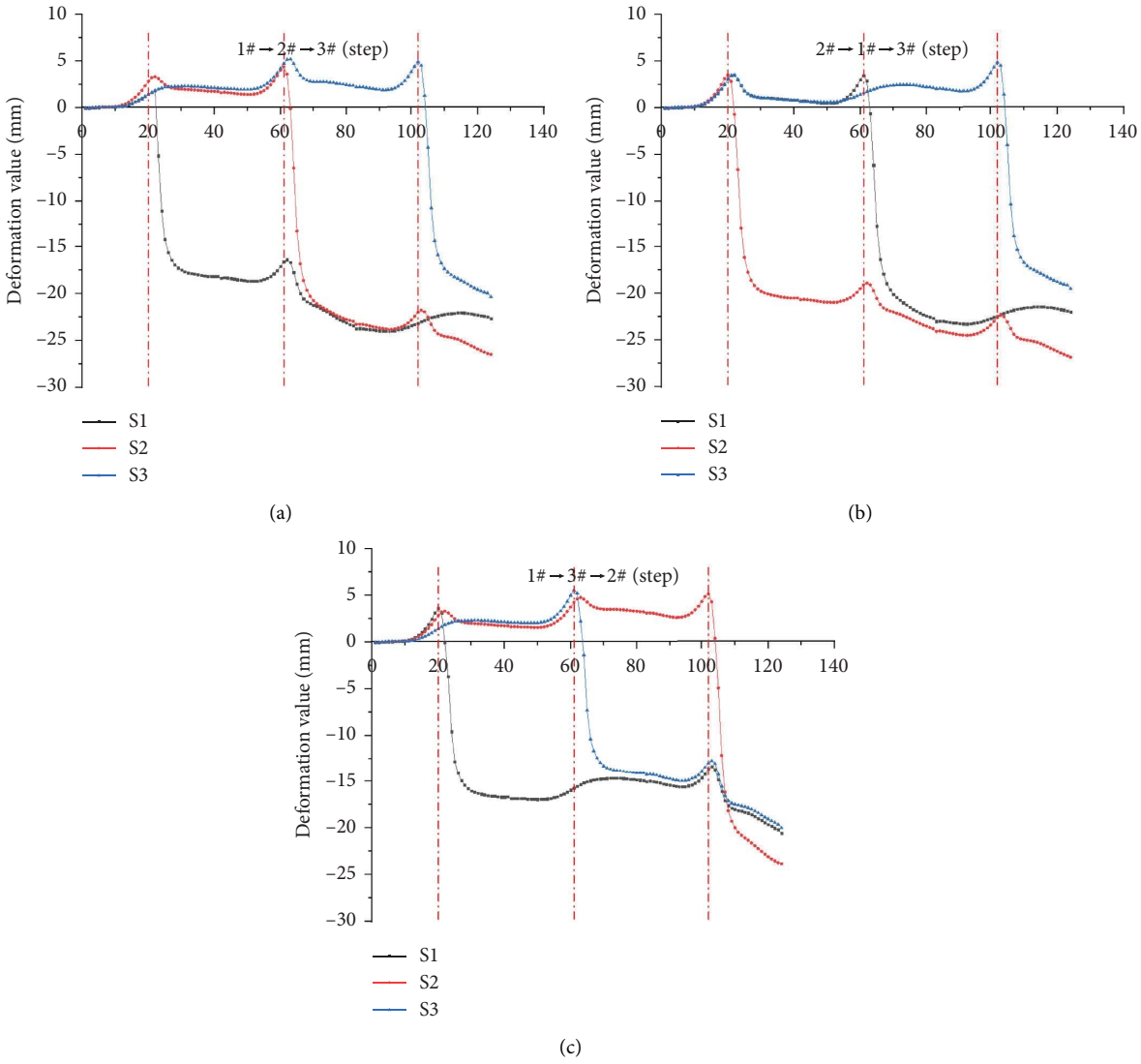

Figure 19: Time-history curve of surface displacement at monitoring points: (a) 1# ⟶ 2# ⟶ 3#; (b) 2# ⟶ 1# ⟶ 3#; (c) 1# ⟶ 3# ⟶ 2#.

maximum values of surface settlement were 26.46 mm, 26.64 mm, and 23.82 mm, respectively.

4.4. Construction Sequence. There was no construction sequence problem of the multiline parallel pipe-jacking in the mutual influence non-self-stability zone and the nonmutual influence self-stability zone. The impact of the multiline parallel pipe-jacking construction in the mutual influence self-stability zone on the surrounding stratum was not that the simple superposition of the individual single-line pipe-jacking construction. Early construction pipe jacking would impact on the surrounding strata of postconstruction pipe jacking by influencing the displacement and stress, while postconstruction pipe jacking would impact on early construction pipe jacking that has been completed during the construction process. Different construction sequence had different impacts on the surrounding strata. Pipe-jacking construction should avoid or reduce the mutual influence of the adjacent pipe-jacking construction as much as possible. Therefore, the reasonable selection of the pipe-jacking construction sequence was related to the safety, efficiency, and even the success or failure of the project construction to a certain extent.

The construction sequence scheme of the multiline parallel pipe-jacking construction for the north city drainage and flood control project through Chu River was established according to the following steps. First, we ensure that technology was feasible, safe, and reliable. Then, the characteristics of stratum deformation caused by the multiline parallel pipe-jacking construction were comparatively analyzed, and the working condition with the minimum stratum deformation was taken. Then, comparative analyses were carried out for construction organization, construction period, project economy, and other factors. Finally, the jacking sequence of "1# ⟶ 3# ⟶ 2#" as the optimal sequence was confirmed. The project was officially launched on June 10 in 2022, and the construction was successfully

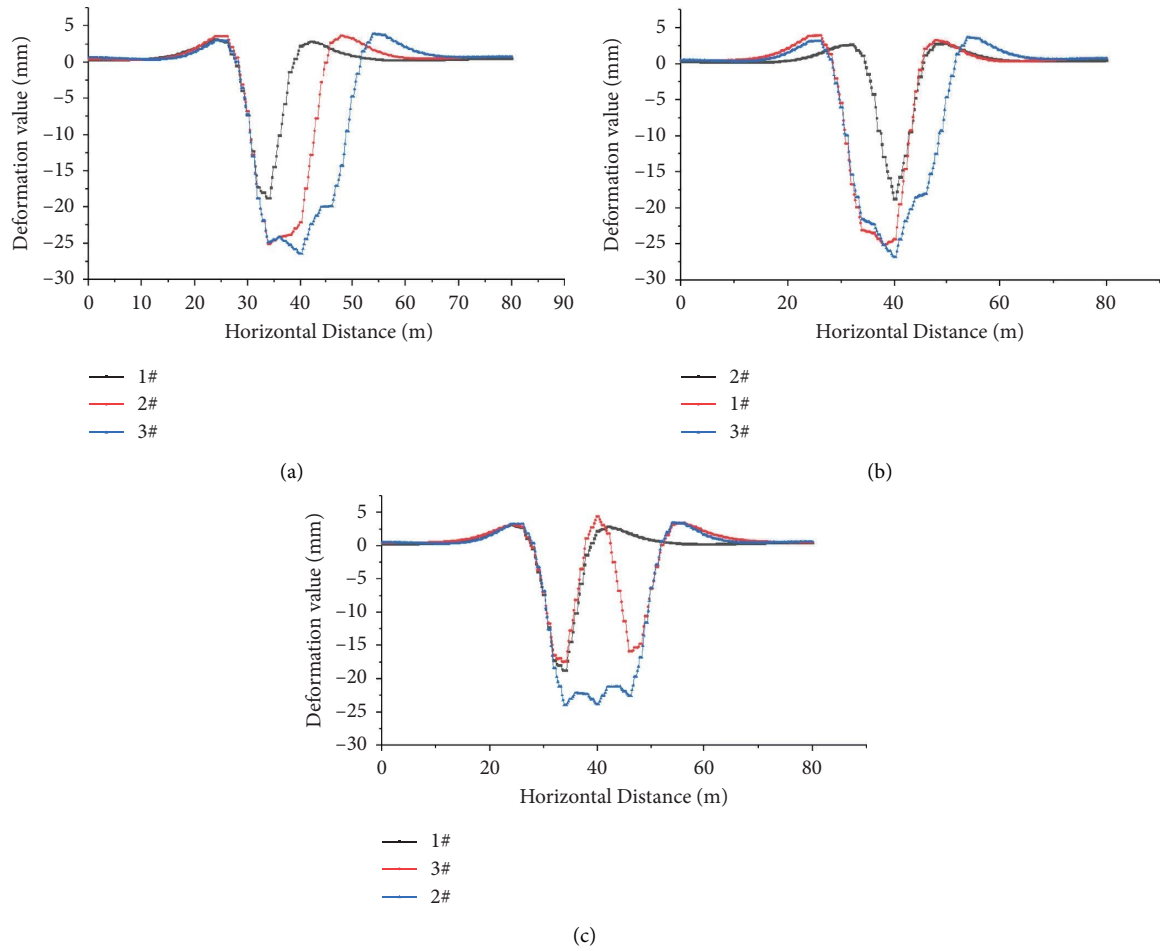

Figure 20: Surface displacement curve of monitoring section: (a) 1# ⟶ 2# ⟶ 3#; (b) 2# ⟶ 1# ⟶ 3#; (c) 1# ⟶ 3# ⟶ 2#.

completed on June 30 in 2022. The project implementation effect was good.

5. Conclusions

(1) It was revealed that the variation law of the surrounding stratum self-stability characteristics for single-line pipe-jacking construction unloading varies with the overburden thickness *Hs*. The surrounding stratum minimum critical overburden thickness $Hs_{\min}$ and the maximum critical overburden thickness $Hs_{\max}$ of single-line pipe-jacking construction unloading were obtained. The surrounding stratum self-stability distribution zone of single-line pipe-jacking construction unloading was drawn, which provided the theoretical basis for the vertical-sectional design of river-crossing pipe jacking with overburden thickness *Hs* drastic change.

(2) It was revealed that the variation law of the surrounding stratum self-stability characteristics for multiline parallel pipe-jacking construction unloading varies with the clear distance *D*. The mathematical fitting equations among the minimum critical clear distance $D_{\min}$, the overburden thickness *Hs*, and the river water depth H_w of multiline parallel pipe-jacking construction unloading were obtained. The spatial feature distribution map among the minimum critical clear distance $D_{\min}$, the overburden thickness *Hs*, and the river water depth H_w was drawn, which provided the theoretical basis for the cross-sectional design of the multiline parallel pipe-jacking construction.

(3) Based on the surrounding stratum self-stability degree and the mutual influence degree of multiline parallel pipe-jacking construction unloading, the surrounding stratum zone was divided into the mutual influence nonself-stability zone, the mutual influence self-stability zone, and the nonmutual influence self-stability zone.

(4) Combined with the relying project, the construction sequence of "1# ⟶ 3# ⟶ 2#" was concluded to be the optimal construction sequence through the comparative analysis of the ground deformation characteristics caused by the multiline parallel pipe-jacking construction and the combination of various factors such as engineering safety, economy, and convenience.

Data Availability

The data used to support the findings of this study are available from the corresponding author upon request.

Conflicts of Interest

The authors declare that they have no conflicts of interest.

Authors' Contributions

Ziguang Zhang was the person in charge of the paper and completed the construction of thesis framework system and thesis writing. Jiesheng Zhang completed the collection, sorting, and analysis of relevant project case data in the paper. Ruijin Mao, Xuefeng Wang, and Mengqing Zhang assisted in completing the related work of numerical calculation in the paper.

Acknowledgments

This study was funded by the Provincial Natural Science Research Project of Colleges and Universities in Anhui Province-Key projects (KJ2021A0611), the Scientific Research Project of Anhui Jianzhu University (no. XJ2019000502), the Science and Technology Plan of Housing and Urban-Rural Construction in Anhui Province (2022-YF096 and 2020-YF38), and the Science and Technology Development Project (HYB20190152, HYB20220092, and HYB20220162).

References

[1] R. L. Sterling, "Developments and research directions in pipe jacking and microtunneling," *Underground Space*, vol. 5, no. 1, pp. 1–19, 2020.

[2] Y. Yuan, Y. S. Xu, A. Arulrajah, and D. J. Yuan"Ground, "Response due to construction of shallow pipe-jacked tunnels in sandy soil: laboratory investigation," *Journal of Testing and Evaluation*, vol. 48, no. 5, pp. 3602–3622, 2020.

[3] K. Wen, W. Zeng, H. Shimada, T. Sasaoka, and A. Hamanaka, "Numerical and theoretical study on the jacking force prediction of slurry pipe jacking traversing frozen ground," *Tunnelling and Underground Space Technology*, vol. 115, Article ID 104076, 2021.

[4] J. Liu, H. Cheng, H. Cai, X. Wang, H. B. Cai, and X. S. Wang, "Design and analysis of grouting pressure in slurry pipe jacking based on the surrounding soil stability mechanical characteristics," *Geofluids*, vol. 2022, Article ID 4697730, 17 pages, 2022.

[5] Q. L. Cui, Y. Xu, S. L. Shen et al., "Field performance of concrete pipes during jacking in cemented sandy silt," *Tunnelling and Underground Space Technology*, vol. 49, pp. 336–344, 2015.

[6] S. L. Shen, Q. L. Cui, C. E. H. Masce, and Y. S. Xu, "Ground response to multiple parallel microtunneling operations in cemented silty clay and sand," *Journal of Geotechnical and Geoenvironmental Engineering*, vol. 142, pp. 1–11, Article ID 04016001, 2016.

[7] C. Wang, J. Liu, H. Cheng, H. Cai, H. Cheng, and H. B. Cai, "Disturbance effect of pipe jacking group adjacent excavation on surrounding soil," *Advances in Civil Engineering*, vol. 2021, Article ID 5533952, 21 pages, 2021.

[8] M. F. Lei, D. Y. Lin, W. C. Yang et al., "Model test to investigate failure mechanism and loading characteristics of shallow-bias tunnels with small clear distance," *Journal of Central South University*, vol. 23, no. 12, pp. 3312–3321, 2016.

[9] A. M. Hefny, H. C. Chua, and J. Y. Zhao, "Parametric studies on the interaction between existing and new bored tunnels," *Tunnelling and Underground Space Technology*, vol. 19, no. 4, pp. 471–483, 2018.

[10] M. Li, X. Zhang, W. Kuang, Z. Zhou, W. Kuang, and Z. Zhou, "Grouting reinforcement of shallow and small clearance tunnel," *Polish Journal of Environmental Studies*, vol. 30, no. 3, pp. 2609–2620, 2021.

[11] S. Cao, S. Huo, A. Guo et al., "Numerical simulation research on the stability of urban underground interchange tunnel group," *Mathematical Problems in Engineering*, vol. 2021, Article ID 9913509, 13 pages, 2021.

[12] C. F. Huang, K. Zhou, B. Deng, D. Li, Q. L. Song, and D. Su, "Influence of construction of the following tunnel on the preceding tunnel in the reinforced soil layer," *Applied Sciences*, vol. 12, no. 20, pp. 10335–10417, 2022.

[13] R. Singh, T. N. Singh, and R. K. Bajpai, "The investigation of twin tunnel stability: effect of spacing and diameter," *Journal of the Geological Society of India*, vol. 91, no. 5, pp. 563–568, 2018.

[14] T. Chen, K. Zhou, J. Wei et al., "Excavation influence of triangular-distribution tunnels for wind pavilion group of a metro station," *Journal of Central South University*, vol. 27, no. 12, pp. 3852–3874, 2020.

[15] J. Ghaboussi and R. E. Ranken, "Interaction between two parallel tunnels," *International Journal for Numerical and Analytical Methods in Geomechanics*, vol. 1, no. 1, pp. 75–103, 1977.

[16] A. Verruijt and J. R. Booker, "Surface settlements due to deformation of a tunnel in an elastic half plane," *Géotechnique*, vol. 46, no. 4, pp. 753–756, 1996.

[17] Y. Wang, D. Zhang, Q. Fang et al., "Analytical solution on ground deformation caused by parallel construction of rectangular pipe jacking," *Applied Sciences*, vol. 12, no. 7, pp. 3298–3320, 2022.

[18] C. Cheng, P. J. Jia, P. P. Ni et al., "Upper bound analysis of longitudinally inclined EPB shield tunnel face stability in dense sand strata," *Transportation Geotechnics*, vol. 41, no. 101031, pp. 101031–101115, 2023.

[19] C. Cheng, H. Yang, P. Jia et al., "Face stability of shallowly buried large-section EPB box jacking crossing the Beijing-Hangzhou Grand Canal," *Tunnelling and Underground Space Technology*, vol. 138, Article ID 105200, pp. 1–22, 2023.

[20] N. Loganathan and H. G. Poulos, "Analytical prediction for tunneling-induced ground movements in clays," *Journal of Geotechnical and Geoenvironmental Engineering*, vol. 124, no. 9, pp. 846–856, 1998.

[21] B. Lu, P. Jia, W. Zhao et al., "Longitudinal mechanical force mechanism and structural design of steel tube slab structures," *Tunnelling and Underground Space Technology*, vol. 132, Article ID 104883, pp. 1–17, 2023.

[22] J. V. Bartlett and B. L. Bubbers, "Surface movements caused by bored tunneling," in *Proceedings of the Conference on Subway Construction*, pp. 513–539, Budapest-Balatonfured, March, 1970.

[23] E. J. Cording and W. H. Hansmire, "Displacements around soft ground tunnel," in *Proceedings of the 5thPan, American*

Conference on Soil Mechanics and Foundation Engineering, vol. 1, no. 4, pp. 571–633, Argentina, July, 1975.

[24] S. Ma, M. Li, J. Jin, K. Bai, J. W. Jin, and K. Bai, "The influence of shallow buried double-line parallel rectangular pipe jacking construction on ground settlement deformation," *Alexandria Engineering Journal*, vol. 60, no. 1, pp. 1911–1916, 2021.

[25] L. J. Tao, Y. Zhang, X. Zhao et al., "Group effect of pipe jacking in silty sand," *Journal of Geotechnical and Geoenvironmental Engineering*, vol. 147, no. 11, pp. 1–14, 2021.

[26] G. B. Shao, N. Yang, and J. Y. Han, "Study on the deformation induced by vertical two-layer large diameter pipe-jacking in the soil-rock composite stratum," *Applied Sciences*, vol. 12, no. 24, pp. 12780–12816, 2022.

[27] L. Ding, G. Shao, J. Shang, J. Han, J. H. Shang, and J. Y. Han, "Study on transverse seismic response characteristics of large diameter vertical double-layer overlapping pipe Jacking in the soil-rock composite stratum," *Applied Sciences*, vol. 13, no. 4, pp. 2343–2414, 2023.

[28] X. M. Du, C. Liu, C. J. Wang et al., "Diffusion characteristics and reinforcement effect of cement slurry on porous medium under dynamic water condition considering infiltration," *Tunnelling and Underground Space Technology*, vol. 130, Article ID 104766, pp. 1–12, 2022.

[29] J. Liang, X. Du, H. Fang et al., "Numerical and experimental study of diffusion law of foamed polymer grout in fracture considering viscosity variation of slurry," *Tunnelling and Underground Space Technology*, vol. 128, Article ID 104674, pp. 1–10, 2022.

[30] K. G. Sun, W. Xu, W. Qiu et al., "Study on the characteristics of safety distribution changing with buried depth for metro station in upper-soft and lower-hard stratum," *Advances in Civil Engineering*, vol. 2018, Article ID 6047919, 14 pages, 2018.

[31] Z. Zhang, T. Xu, G. Cao, X. Liu, G. Y. Xu, and X. F. Liu, "Distribution features of the minimum rock cover thickness of the surrounding rock self-stability of the metro tunnel in the soil-rock dualistic stratum," *Advances in Civil Engineering*, vol. 2020, Article ID 9120983, 12 pages, 2020.

[32] P. Zhou, Y. Jiang, F. Zhou et al., "Stability evaluation method and support structure optimization of weak and fractured slate tunnel," *Rock Mechanics and Rock Engineering*, vol. 55, no. 10, pp. 6425–6444, 2022.

[33] Y. G. Zhang, S. Kai, H. Z. Zhu, Z. D. Qian, and H. G. Yu, "Installation time of an initial support for tunnel excavation upon the safety factors of surrounding rock," *Applied Sciences*, vol. 10, pp. 1–17, 2020.

[34] X. Zhang, M. Wang, J. Li et al., "Safety factor analysis of a tunnel face with an unsupported span in cohesive frictional soils," *Computers and Geotechnics*, vol. 117, pp. 103221–103229, 2020.

[35] Q. Li, R. Li, W. He et al., "Characteristics of dynamic safety factors during the construction process for a tunnel-group metro station," *Applied Sciences*, vol. 12, no. 10, pp. 4900–4912, 2022.

[36] Q. Jiang, X. Liu, F. Yan et al., "Failure performance of 3DP physical twin-tunnel model and corresponding safety factor evaluation," *Rock Mechanics and Rock Engineering*, vol. 54, no. 1, pp. 109–128, 2021.